HHS Public Access

Author manuscript

Bioorg Med Chem Lett. Author manuscript; available in PMC 2022 December 01.

Published in final edited form as:

Bioorg Med Chem Lett. 2021 December 01; 53: 128416. doi:10.1016/j.bmcl.2021.128416.

Discovery of structurally distinct tricyclic M_4 positive allosteric modulator (PAM) chemotypes - Part 2

Madeline F. Long[a,b,1], **Rory A. Capstick**[a,b,1], **Paul K. Spearing**[a,b], **Julie L. Engers**[a,b], **Alison R. Gregro**[a,b], **Sean R. Bollinger**[a,b], **Sichen Chang**[a,b], **Vincent B. Luscombe**[a,b], **Alice L. Rodriguez**[a,b], **Hyekyung P. Cho**[a,b], **Colleen M. Niswender**[a,b,d,e,f], **Thomas M. Bridges**[a,b], **P. Jeffrey Conn**[a,b,d,e,f], **Craig W. Lindsley**[a,b,c,f], **Darren W. Engers**[a,b], **Kayla J. Temple**[a,b,*]

[a]Warren Center for Neuroscience Drug Discovery, Vanderbilt University, Nashville, TN 37232, USA

[b]Department of Pharmacology, Vanderbilt University School of Medicine, Nashville, TN 37232, USA

[c]Department of Chemistry, Vanderbilt University, Nashville, TN 37232, USA

[d]Vanderbilt Kennedy Center, Vanderbilt University Medical Center, Nashville, TN 37232, USA

[e]Vanderbilt Brain Institute, Vanderbilt University School of Medicine, Nashville, TN 37232, USA

[f]Vanderbilt Institute of Chemical Biology, Vanderbilt University School of Medicine, Nashville, TN 37232, USA

Abstract

This Letter details our efforts to develop novel tricyclic M_4 PAM scaffolds with improved pharmacological properties. This endeavor involved a “tie-back” strategy to replace the 3-amino-4,6-dimethylthieno[2,3-b]pyridine-2-carboxamide core which lead to the discovery of two novel tricyclic cores: a 7,9-dimethylpyrido[3’,2’:4,5]thieno[3,2-d]pyrimidine core and 2,4-dimethylthieno[2,3-b:5,4-c’]dipyridine core. Both tricyclic cores displayed low nanomolar potency against the human M_4 receptor.

Graphical Abstract

*Corresponding author at Warren Center for Neuroscience Drug Discovery at Vanderbilt University, Vanderbilt University, Nashville, TN 37232, USA. kayla.temple@vanderbilt.edu (K.J. Temple).

[1]These authors contributed equally to this work.

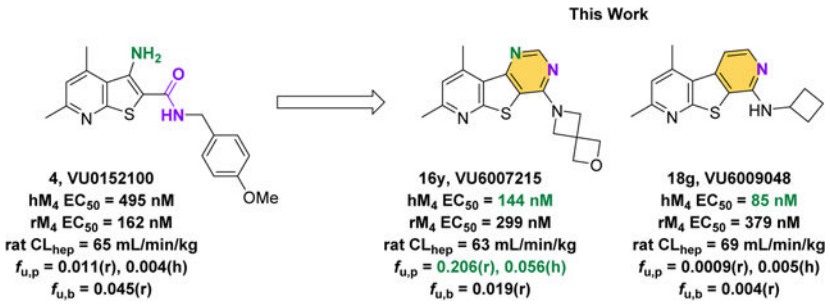

Keywords

M_4; Muscarinic acetylcholine receptor; Positive Allosteric modulator (PAM); Structure Activity Relationship (SAR)

Muscarinic acetylcholine receptor subtype 4 (M_4) positive allosteric modulators (PAMs) continue to be important drug targets as novel treatments for various neurological disorders such as Parkinson's disease,[1] Huntington's disease,[2] and schizophrenia (both the positive and negative symptom clusters).[3–7] Classically, M_4 PAMs possess a β-amino carboxamide moiety as a key pharmacophore (circled in **2**, Figure 1) which was believed to be essential for M_4 PAM activity.[8–14] As such chemotypes have been plagued with poor solubility, varying degrees of P-gp efflux, and potency differences across species, efforts have been made to develop M_4 PAM chemotypes devoid of the β-amino carboxamide moiety.[3,14–26] Clinical studies featuring xanomeline, a M_1/M_4 preferring agonists that lacks the β -amino carboxamide moiety, have validated targeting the muscarinic cholinergic system as a method for treating the psychosis and behavioral disturbances observed in both Alzeheimer's and schizophrenia patients.[23,24] However, the lack of receptor subtype selectivity resulted in undesired side effects which ultimately lead to a discontinuation of clinical development. An effort to circumvent these adverse events led to the development of KarXT which is currently undergoing clinical trials. KarXT is a treatment in which xanomeline is co-administered with a pan-selective peripheral muscarinic acetylcholine receptor antagonist (trospium) to minimize the adverse side effects of xanomeline.[25] Additional work in the field led to the identification of a selective M_4 PAM which lacked the β-amino carboxamide moiety. Not only was this PAM efficacious in preclinical assays but had fewer and less severe adverse cholinergic-related side effects than observed in rats treated with the nonselective M_4 agonist xanomeline.[26] This indicates that receptor-subtype-selective M_4 PAMs could potentially improving safety profiles. In fact, CVL-231 (a selective M_4 PAM) is currently undergoing clinical trials.[27,28]

Our laboratory previously described two structurally distinct 5,6,6-tricyclic scaffolds devoid of the β-amino carboxamide moiety that afforded potent and CNS penetrant M_4 PAMs.[17] In an effort to identify additional novel M_4 PAM chemotypes, we employed a "tie-back" strategy in order to mask the β-amino carboxamide moiety of one of our early lead M_4 PAM compounds, **VU0152100**.[10–11] When designing this new scaffold, we elected to keep the 4,6-dimethylthieno[2,3-*b*]pyridine core intact while masking the β-amino carboxamide as a pyrimidine moiety, a strategy utilized in the development of

VU6017654 (3). This resulted in the discovery of a novel M_4 PAM chemotype containing a 7,9-dimethylpyrido[3',2':4,5]thieno[3,2-d]pyrimidine core, **5**. Further exploration revealed a second novel, tricyclic M_4 PAM chemotype containing a 2,4-dimethylthieno[2,3-b:5,4-c']-dipyridine core, **6**. This body of work details the development of these two novel M_4 PAM chemotypes.

The synthesis of core **5** began with the commercially available amine **7**, which was first condensed with formamide followed by formamidine acetate salt to afford the pyrimidone intermediate **9** (Scheme 1). Treatment of pyrimidone **9** with $POCl_3$ gave chloride **11** which readily underwent nucleophilic aromatic substitution with a variety of primary and secondary amines as well as alcohols to yield desired analogs **16** and **19**. For this exercise, we chose to evaluate benzyl amines and amino azetidines that proved to be successful in our past endeavors to afford potent M_4 PAMs.[15–17,29]

Select analogs **16** & **19** were screened against the human M_4 (hM_4) receptor to determine potency with results highlighted in Table 1. It became very clear that the amine "tail" greatly influences potency. It was noted that minor changes, such as a fluoro-substitution on the phenyl ring (**16m** vs. **16n**), led to a ~2.5-fold decrease in potency. Moreover, removal of one fluorine from the trifluoromethoxy group of **16d** (inactive) afforded analog **16e** (EC_{50} = 4 μM), which reestablished activity at hM_4. Another intriguing finding was observed when the amine linker (**16m;** hM_4 EC_{50} = 910 nM) was exchanged for an ether linker (**19;** hM_4 EC_{50} = 8.7 μM) resulting in a 9.6-fold loss of potency.

Noting the importance of the amine "tail", we next elected to explore small aliphatic amines (Table 2) as well as small carbon-linked groups (Table 3) which were synthesized in accordance with Scheme 2. Briefly, commercially available 2-mercapto-4,6-dimethyl nicotinonitrile (**22**) was condensed with various α-bromo ketones in a Gewald-type reaction to afford thieno[2,3-*b*] pyridines **23**. As previously described in Scheme 1, condensation with formamide afforded final compounds **24**. The piperidine intermediate **24e** could be further transformed via nucleophilic aromatic substitutions (**26**), HATU-assisted amide formation (**28**), or reductive amination (**30**). Finally, the synthesis of biaryl analog **21** was accomplished utilizing intermediate **11** in a Stille cross-coupling reaction as described in Scheme 1.

Select analogs 1**6s-y**, **21**, **24, 26**, **28**, and **30** were screened against human M_4 (hM_4) to determine potency with results highlighted in Tables 2 & 3. Selecting small amines as our "tail" groups (**16s-y**) proved most advantageous as the majority of analogs in Table 2 possess hM_4 PAM functional potencies less than 500 nM, with three analogs displaying EC_{50}'s < 300 nM: **16w** (hM_4 EC_{50} = 277 nM), **16x** (hM_4 EC_{50} = 172 nM), and **16y** (hM_4 EC_{50} = 144 nM).

Conversely, similar small carbon-linked tail groups resulted in a loss of hM_4 functional potency (Table 3): **21** (hM_4 EC_{50} = 3.4 μM**), 24a** (hM_4 EC_{50} = 6.8 μM), **24b** (hM_4 EC_{50} = 3.9 μM), **24c** (hM_4 EC_{50} = 2.8 μM). Most notably, the addition of a hydrogen bond acceptor into the cyclohexyl ring of analog **24a** to give the tetrahydropyran analog **24d** (hM_4 EC_{50} = 152 nM), resulted in a nearly 45-fold increase in hM_4 functional potency.

Comparison of **24d** to the corresponding piperidine analog **24e** (hM_4 EC_{50} = 6.1 μM) once again resulted in a loss of hM_4 functional potency (~40-fold). To investigate the importance of a hydrogen bond acceptor at this position, we further investigated the piperidine tail by eliminating its ability to serve as a hydrogen bond donor. This exercise generated amides (**28a** & **28b**), small aliphatic C-linked piperidines (**30**), as well as aryl-linked piperidines (**26**). Interestingly, converting piperidine **24e** into amides **28a** (hM_4 EC_{50} = 620 nM) and **28b** (hM_4 EC_{50} = 234 nM) led to an increase in functional M_4 potency by ~10-fold and 26-fold, respectively. Removing the carbonyl of analog **28a** to afford analog **30** resulted in a complete loss of M_4 potency, further supporting our theory of the importance of a hydrogen bond acceptor at this position. Similarly, a complete loss of activity was observed when the piperidine tail of **24e** was capped with 3-fluoropyridine (**26**). This loss of activity could be attributed to several factors including the large size of the C-linked “tail”, the position/orientation of the electron lone pair of the pyridine, and/or the effects of the fluorine substituent on the basicity of the pyridine.

After extensive exploration of the amine tail, we turned our attention toward accessing the importance of the sulfur of the 7,9-dimethylpyrido[3’,2’:4,5]thieno[3,2-d]pyrimidine core. To do so, we exchanged the sulfur with an oxygen to generate a 7,9-dimethylpyrido[3’,2’:4,5]furo[3,2-d]pyrimidine core, **17**. Similar to the synthesis **16**, the synthesis of core **17** began by condensing formamide with ethyl 3-amino-4,6-dimethylfuro[2,3-b]pyridine-2-carboxylate (**8**) to afford the pyrimidone intermediate **10** (Scheme 1). Treatment of pyrimidone **10** with $POCl_3$ gave chloride **12** which readily underwent nucleophilic aromatic substitution with a variety of primary and secondary amines to afford desired analogs **17** in moderate to good yields.

Functional hM_4 potencies for analogs **17** were determined and the results highlighted in Table 4. Of the compounds evaluated, none possessed sub-micromolar potencies. In fact, we observed complete loss of activity in several analogs (**17a**, **17d**, **17e**, and **17f**). Directly comparing analog **16m** (hM_4 EC_{50} = 910 nM) to **17e** (inactive), **16w** (hM_4 EC_{50} = 277 nM) to **17a** (inactive), and **16v** (hM_4 EC_{50} = 359 nM) to **17c** (hM_4 EC_{50} = 1.59 μM; 4.4-fold potency decrease) further illustrates the significance of the sulfur atom in the tricyclic ring.

Finally, we evaluated the relevance of the pyrimidine nitrogen at the 5-position by synthesizing analogs **18** (Scheme 1). These analogs were synthesized from commercially available amine **7**, which underwent a Sandmeyer reaction to give the corresponding bromide. The bromide intermediate was transformed into intermediate **13** via a Suzuki cross-coupling reaction. Cyclization of **13** to form the pyrone followed by exchange with ammonia afforded the pyridone **14**, which was chlorinated via treatment with $POCl_3$ to give intermediate **15** in moderate to good yields. Chloride **15** then underwent nucleophilic aromatic substitution with varies amines to give analogs **18**.

Analogs **18** were screened against hM_4 to determine potency with results highlighted in Table 5. It was immediately apparent that this modification was not detrimental to hM_4 activity. In fact, several analogs displayed increased potencies. For instance, direct comparisons between **16m** (hM_4 EC_{50} = 910 nM) and **18b** (hM_4 EC_{50} = 327 nM) resulted in a ~2.8-fold increase in potency. Similarly, comparing **16p** (hM_4 EC_{50} = 6.55 μM) and **18c**

(hM_4 EC_{50} = 150 nM) resulted in a ~44-fold increase in potency. Likewise, this trend was also observed when analyzing **16v** (hM_4 EC_{50} = 359 nM) and **18g** (hM_4 EC_{50} = 85 nM) which resulted in a ~4-fold increase in functional hM_4 potency.

Of these compounds, **16o**, **16w**, **16x**, **16y**, **28b**, **18b**, **18d**, and **18g** were advanced into a battery of *in vitro* DMPK assays and our standard rat plasma:brain level (PBL) cassette paradigm (Table 6).[18] These compounds were chosen to move forward based on their M_4 potency (EC_{50} < 350 nM) as well as their chemical diversity across subseries. In regard to physicochemical properties, these analogs all possessed molecular weights less than 450 Da possessed molecular weights less than 450 Da with **16o**, **16w**, and **16x** having the most attractive CNS xLogP values (2.79 – 3.39).[30–31] All analogs tested displayed high predicted hepatic clearance in at least one species based on microsomal CL_{int} data (rat CL_{hep}s > 56 mL/min/kg). While analogs **16o** and **28b** displayed moderate human predicted hepatic clearance based on microsomal CL_{int} data (human CL_{hep}s of 11–12 mL/min/kg) all other analogs tested displayed high human predicted hepatic clearance based on microsomal CL_{int} data (human CL_{hep} > 15 mL/min/kg).

Compounds within the tricycle series of core **6** (**18b**, **18d**, & **18g**) were, in general, highly bound to plasma protein (rat f_us plasma 0.005 – 0.016; rat f_us brain 0.002 – 0.004; human f_us plasma 0.001 – 0.005). By contrast, compounds within the tricyclic series of core **5** (**16o**, **16w**, **16x**, **16y**, **28b**) exhibited reduced protein binding profiles (rat f_us plasma 0.017 – 0.21; rat f_us brain 0.004 – 0.019; human f_us plasma 0.002 – 0.056). Interestingly, compounds **16y** and **28b** displayed the best overall protein binding profiles (rat f_us 0.017 – 0.21; rat f_us brain 0.032 – 0.053; human f_us 0.011 – 0.019); however, these analogs were not progressed forward due to their high predicted hepatic clearance in rat and/or human. Analogs **16o** (rat brain:plasma K_p = 0.45, $K_{p,uu}$ = 0.21) and **16x** (rat brain:plasma K_p = 6.49, $K_{p,uu}$ = 0.27) proved to have low CNS distribution of unbound drug, while analogs **16w**, **16y** and **28b** displayed moderate CNS distribution (rat $K_{p,uu}$s = 0.35 – 0.65). On the other hand, analogs **18d** (rat brain:plasma K_p = 37.1, $K_{p,uu}$ = 4.87) and **18g** (rat brain:plasma K_p = 10.4, $K_{p,uu}$ = 4.18) displayed excellent CNS penetration; however, these compounds suffered from low fraction unbound.

In summary, a scaffold hopping exercise utilizing a “tie-back” strategy based on M_4 PAM **3** proved to be a successful strategy in converting an early lead compound, **VU0152100,** into potent tricyclic M_4 PAM analogs devoid of the classic β-amino carboxamide moiety. Analogs within the tricycle series containing the 2,4-dimethylthieno[2,3-b:5,4-c’]dipyridine core (**6**) gave many potent M_4 PAMs (Table 5; hM_4 EC_{50} = 85–327 nM); however, these analogs displayed very poor fraction unbound in regards to brain and plasma protein (f_us < 0.01) as well as high human (CL_{hep}s ≥ 15 mL/min/kg) and rat (CL_{hep}s ≥ 60 mL/min/kg) predicted hepatic clearance. Thus, additional analogs of core **6** were not pursued further. Directing our effort toward the 7,9-dimethylpyrido[3’,2’:4,5]thieno[3,2-d]pyrimidine core (**5**) showed benzyl amine linked analogs generally provide only moderately potent analogs (Table 1). Changing the linker to small aliphatic amine linkers provided several potent M_4 PAMs (Table 2; hM_4 EC_{50} = 144–453 nM). On further evaluation, this subseries of analogs generally exhibited improved plasma protein binding profiles. Unfortunately, the small aliphatic amine linker analogs suffered from very high human (CL_{hep}s ≥ 18 mL/min/kg)

and rat (CL_{hep}s ≥ 62 mL/min/kg) predicted hepatic clearance and further work on this subseries was abandoned. Further exploration revealed that carbon-linked groups (Table 3) showed improved brain and plasma f_us when compared to the 2,4-dimethylthieno[2,3-b:5,4-c']dipyridine core (**6**) as previously discussed; however, due to poor human and rat predicted hepatic clearance, further work on this subset of analogs was not pursued.

Our efforts to mask the β-amino carboxamide moiety of an early lead M_4 PAM compound, **VU0152100**, resulted in the discovery of two new tricyclic cores (**5** & **6**) which provided potent M_4 PAM analogs. This endeavor also provided analogs **VU6007215** & **VU6009048**, which display 3.5- fold and 6-fold increase in human M_4 activity, respectively, when compared to parent compound **VU0152100**. Moreover, **VU6007215** exhibits a reduced protein binding profile in relation to the parent compound **VU0152100**. In comparison to the previously reported **VU6017654** (rat f_us plasma 0.007; rat f_us brain 0.003; human f_us plasma 0.021), **VU6007215** shows a much-improved protein binding profile (rat f_us plasma 0.206; rat f_us brain 0.019; human f_us plasma 0.056). Additionally, **VU6007215** displayed higher CNS distribution of unbound drug (rat brain:plasma K_p = 4.47, $K_{p,uu}$ = 0.40) than that of **VU6017654** (rat brain:plasma K_p = 0.25, $K_{p,uu}$ = 0.11); however, a ~2-fold loss in hM_4 and rM_4 functional potency was observed with **VU6007215**. Although this excursion did not deliver PAMs with DMPK profiles to warrant advancement as development candidates, it did garner insights for future scaffold designs toward that goal. These refinements will be reported in due course.

Acknowledgments

We thank the NIH for funding via the NIH Roadmap Initiative 1X01 MH077607 (C.M.N.), the Molecular Libraries Probe Center Network (U54MH084659 to C.W.L.) and U01MH087965 (Vanderbilt NCDDG). We also thank William K. Warren, Jr. and the William K. Warren Foundation who funded the William K. Warren, Jr. Chair in Medicine (to C.W.L.).

References and Notes

1. Shen W, Plotkin JL, Francardo V, et al. M_4 Muscarinic receptor signaling ameliorates striatal plasticity deficits in models of L-DOPA-induced dyskinesia. Neuron. 2015;88:762–773. [PubMed: 26590347]
2. Pancani T, Foster DJ, Moehle MS, et al. Allosteric activation of M_4 muscarinic receptors improve behavioral and physiological alteration in early symptomatic YAC128 mice. Proc Natl Acad Sci USA. 2015;112:14078–14083. [PubMed: 26508634]
3. Bridges TM, LeBois EP, Hopkins CR, et al. The Antipsychotic potential of muscarinic allosteric modulation. Drug News Perspect. 2010;23:229–240. [PubMed: 20520852]
4. Foster DJ, Wilson JM, Wess J, et al. Antipsychotic-like effects of M_4 positive allosteric modulators are mediated by CB_2 receptor-dependent inhibition of Dopamine release. Neuron. 2016;91:1244–1252. [PubMed: 27618677]
5. Jones CK, Byun N, Bubser M. Muscarinic and nicotinic acetylcholine receptor agonists and allosteric modulators for the treatment of Schizophrenia. Neuropsychopharmacology. 2012;37:16–42. [PubMed: 21956443]
6. Farrell M, Roth BL. Allosteric Antipsychotics: M_4 Muscarinic potentiators as novel treatments for Schizophrenia. Neuropsychopharmacology. 2010;35:851–852. [PubMed: 20145632]
7. Kruse AC, Kobilka BK, Gautam D, et al. Muscarinic acetylcholine receptors: novel opportunities for drug development. Nat Rev Drug Discov.2014;13: 549–560. [PubMed: 24903776]

8. Chan WY, McKinzie DL, Bose S, et al. Allosteric modulation of the muscarinic M_4 receptor as an approach to treating Schizophrenia. Proc Natl Acad Sci USA. 2008;105:10978–10983. [PubMed: 18678919]
9. Leach K, Loiacono RE, Felder CC, et al. Molecular Mechanisms of action and *in vivo* validation of an M_4 muscarinic acetylcholine receptor allosteric modulator with potential antipsychotic properties. Neuropsychopharmacology. 2010;35:855–869. [PubMed: 19940843]
10. Brady A, Jones CK, Bridges TM, et al. Centrally active allosteric potentiators of the M_4 muscarinic acetylcholine receptor reverse amphetamine-induced hyperlocomotor activity in rats. J Pharm Exp Ther. 2008;327;941–953.
11. Byun NE, Grannan M, Bubser M, et al. Antipsychotic drug-like effects of the selective M_4 muscarinic acetylcholine receptor positive allosteric modulator VU0152100. Neuropsychopharmacology. 2014;39:1578–1593. [PubMed: 24442096]
12. Bubser M, Bridges TM, Dencker D, et al. Selective activation of M_4 muscarinic acetylcholine receptors reverses MK-801-induced behavioral impairments and enhances associative learning in rodents. ACS Chem Neurosci. 2014;5:920–942. [PubMed: 25137629]
13. Melancon BJ, Wood MR, Noetzel MJ, et al. Optimization of M_4 positive allosteric modulators (PAMs): The discovery of VU0476406, a non-human primate *in* vivo tool compound for translational pharmacology. Bioorg Med Chem Lett. 2017;27:2296–2301. [PubMed: 28442253]
14. Wood MR, Noetzel J, Melancon BH, et al. Discovery of VU0467485/AZ13713945: An M_4 PAM evaluated as a preclinical candidate for the treatment of Schizophrenia. ACS Med Chem Lett. 2017;8:233–238. [PubMed: 28197318]
15. Temple KJ, Engers JL, Long MF, et al. Discovery of a novel 3,4-dimethylcinnoline carboxamide M_4 positive allosteric modulator (PAM) chemotype via scaffold hopping. Bioorg Med Chem Lett. 2019;29:126678. [PubMed: 31537424]
16. Temple KJ, Engers JL, Long MF, et al. Discovery of a novel 2,3-dimethylimidazo[1,2-a]pyrazine-6-carboxamide M_4 positive allosteric modulator (PAM) chemotype. Bioorg Med Chem Lett. 2020;30:126812. [PubMed: 31784320]
17. Temple KJ, Long MF, Engers JL, et al. Discovery of structurally distinct tricyclic M_4 positive allosteric modulator (PAM) chemotypes. Bioorg Med Chem Lett. 2020;30:126811. [PubMed: 31787491]
18. Tarr JC, Wood MR, Noetzel MJ, et al. Challenges in the development of an M_4 PAM preclinical candidate: The discovery, SAR, and *in vivo* characterization of a series of 3-aminoazetidine-derived amides. Bioorg Med Chem Lett.2017;27:2990–2995. [PubMed: 28522253]
19. Le U, Melancon BJ, Bridges TM, et al. Discovery of a selective M_4 positive allosteric modulator based on 3-amino-thieno[2,3- *b*]pyridine-2-carboxamide scaffold: Development of ML253, a potent and brain penetrant compound that is active in a preclinical model of schizophrenia. Bioorg Med Chem Lett. 2013;23:346–350. [PubMed: 23177787]
20. Kennedy JP, Bridges TM, Gentry PR, et al. Synthesis of Structure-Activity Relationships of Allosteric Potentiators of the M_4 Muscarinic Acetylcholine Receptor. ChemMedChem. 2009;4:1600–1607. [PubMed: 19705385]
21. Salovich JM, Vinson PN, Sheffler DJ. Discovery of *N*-(4-methoxy-7-methylbenzo[*d*]thiazol—2-yl)isonicotinamide, ML293, as a novel, selective and brain penetrant positive allosteric modulator of the muscarinic 4 (M_4) receptor. Bioorg Med Chem Lett. 2012;22:5084–5088. [PubMed: 22738637]
22. Smith E, Peter C, Niswender CM. Application of Parallel Multiparametric Cell-Based FLIPR Detection Assays for the Identification of Modulators of the Muscarinic Acetylcholine Receptor 4 (M_4). Biomol Screening. 2015;20:858–868.
23. Bodick NC, Offen WW, Levey AI, et al. Effects of xanomeline, a selective muscarinic receptor agonist, on cognitive function and behaviorl symptoms in Alzheimer disease. Arch Neurol. 1997;54:465–473. [PubMed: 9109749]
24. Shekhar A, Potter WZ, Lightfoot J, et al. Selective muscarinic receptor agonist xanomeline as a novel treatment approach for schizophrenia. Am J Psyciatry. 2018;165:1033–1039.
25. Brannan SK, Sawchak S, Miller AC, et al. Muscarinich Cholinergic Receptor Agonist and Peripheral Antagonist for Schizophrenia. N Engl J Med. 2021;384:717–726. [PubMed: 33626254]

26. Schuber JW, Harrison ST, Mulhearn J, et al. Discovery, Optimization, and Biological Characterization of 2,3,6-Trisubstituted Pyridine-Containing M4 Positive Allosteric Modulators. ChemMedChem. 2019:14:943–951. [PubMed: 30920765]
27. https://clinicaltrials.gov/ct2/show/NCT04136873. A Multiple Ascending Dose Trial of CVL-231 in Subjects with Schizophrenia. Date of Access: 10/11/2021
28. https://clinicaltrials.gov/ct2/show/NCT04787302?term=CVL-231. PET Trial to Evaluate Target Occupancy of CVL-231 on Brain Receptors Following Oral Dosing. Date of Access: 10/11/2021
29. Long MF, Engers JL, Chang S, et al. Discovery of a novel 2,4-dimethylquinolin-6-carboxamide M_4 positive allosteric modulator (PAM) chemotype via scaffold hopping. Bioorg Med Chem Lett. 2017;27:4999–5001. [PubMed: 29037946]
30. Rankovic Z CNS Drug Design: Balancing Physiochemical Properties for Optimal Brain Exposure. J Med Chem. 2015;58:2584–2608. [PubMed: 25494650]
31. Wager TT, Hou X, Verhoest PR, et al. Central Nervous System Multiparameter Optimization Desirability: Application in Drug Discovery. ACS Chem Neurosci. 2016;7:767–775. [PubMed: 26991242]

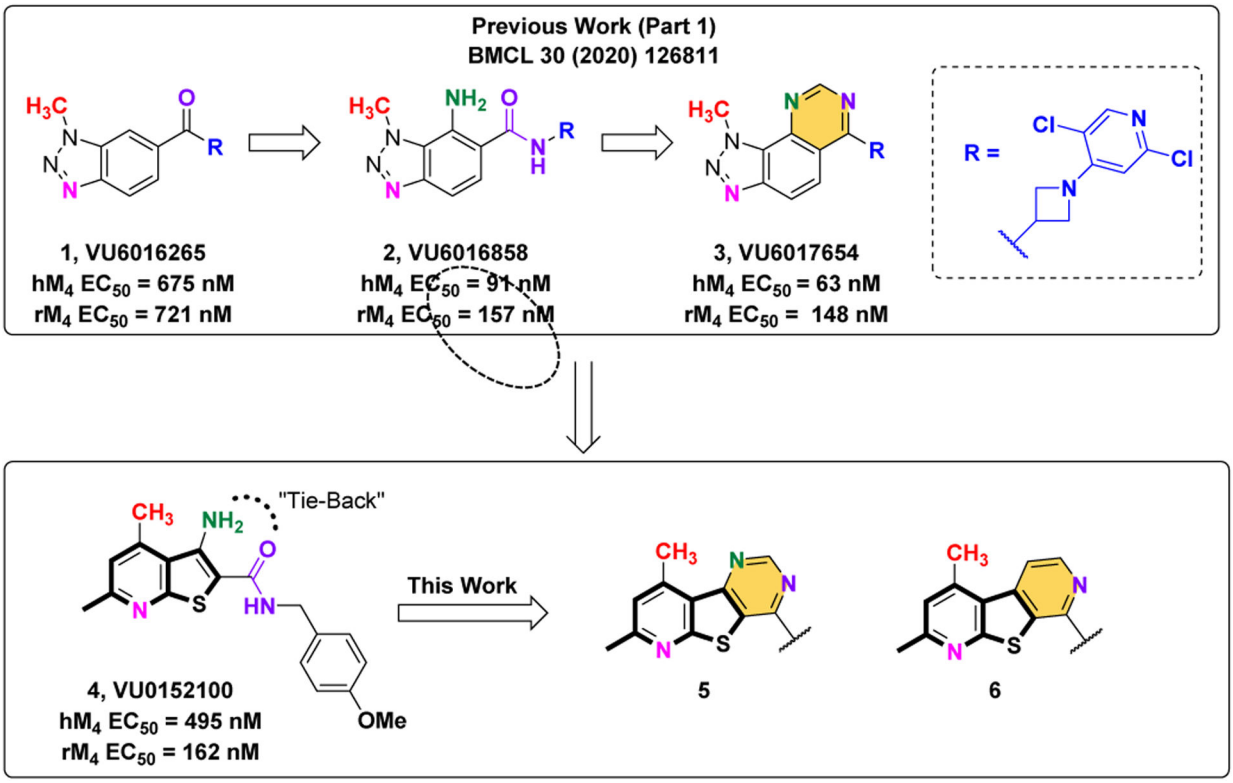

Figure 1.

Exploration of novel tricyclic cores as M_4 PAMs. We utilized the same "tie-back" strategy to mask the β-amino carboxamide moiety (dotted circle), which contributed to the discovery of **VU6017654** (**3**), to develop two unique M_4 PAM tricyclic chemotypes: a 7,9-dimethylpyrido[3',2':4,5]thieno[3,2-d]pyrimidine core (**5**) and a 2,4-dimethylthieno[2,3-b:5,4-c']dipyridine core (**6**).

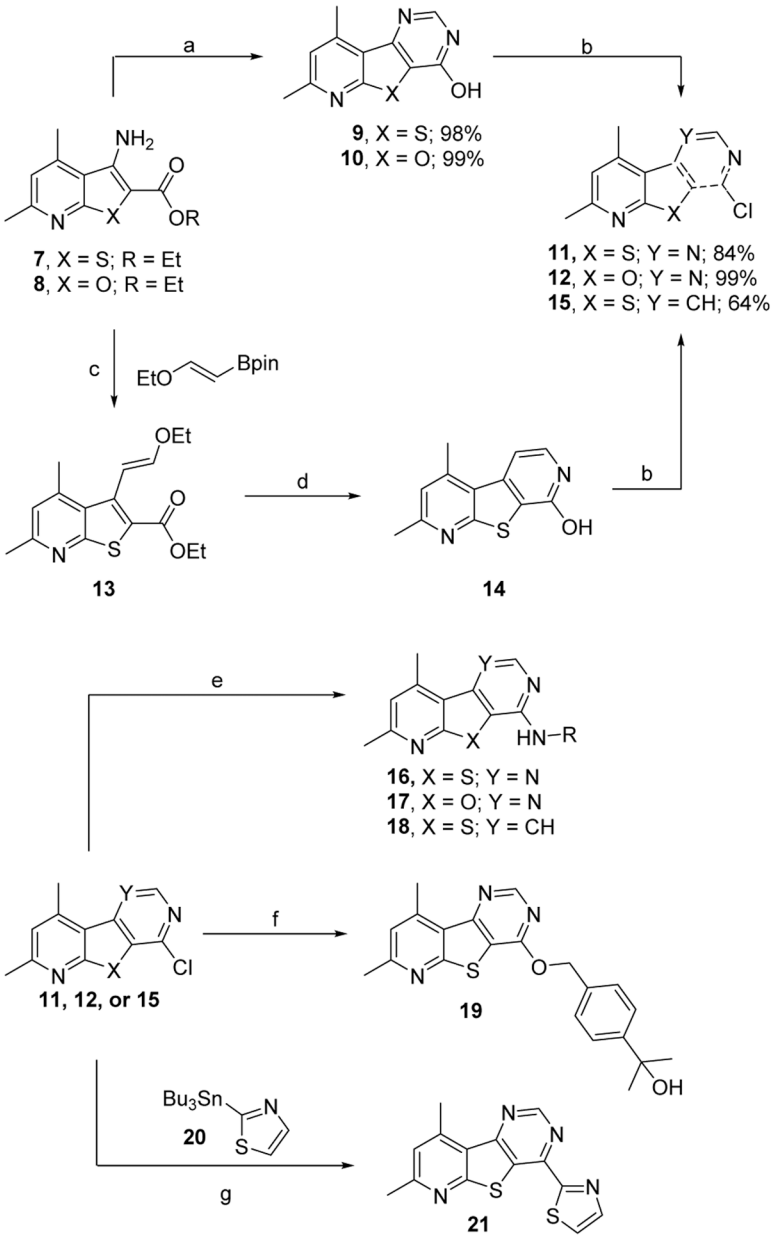

Scheme 1.

Synthesis of M_4 PAM analogs. Reagents and conditions: (a) i. $HCONH_2$, 150 °C; ii. AcOH • $HN{=}CHNH_2$, 150 °C; (b) $POCl_3$, 120 °C, 18h; (c) i. $CuBr_2$, ^{t}BuONO, CH_3CN, 60 °C, 56%; ii. Cs_2CO_3, $Pd(dppf)Cl_2$, dioxane/H_2O (10:1), 90 °C, 18h, 99%; (d) i. TFA, 100 °C, 4h, 98%; ii. NH_4OH, 100 °C, 48h, 98%; (e) amine, DIEA, NMP, 120 °C, 21–88%; (f) i. Methyl (4-hydroxymethyl)benzoate, NaH, THF, 0 °C, 17%; ii. MeMgBr, THF, 0 °C, 38%; (g) **20**, $Pd(PPh_3)_4$, 1,4-dioxane, μW 120 °C, 0.5h, 10%.

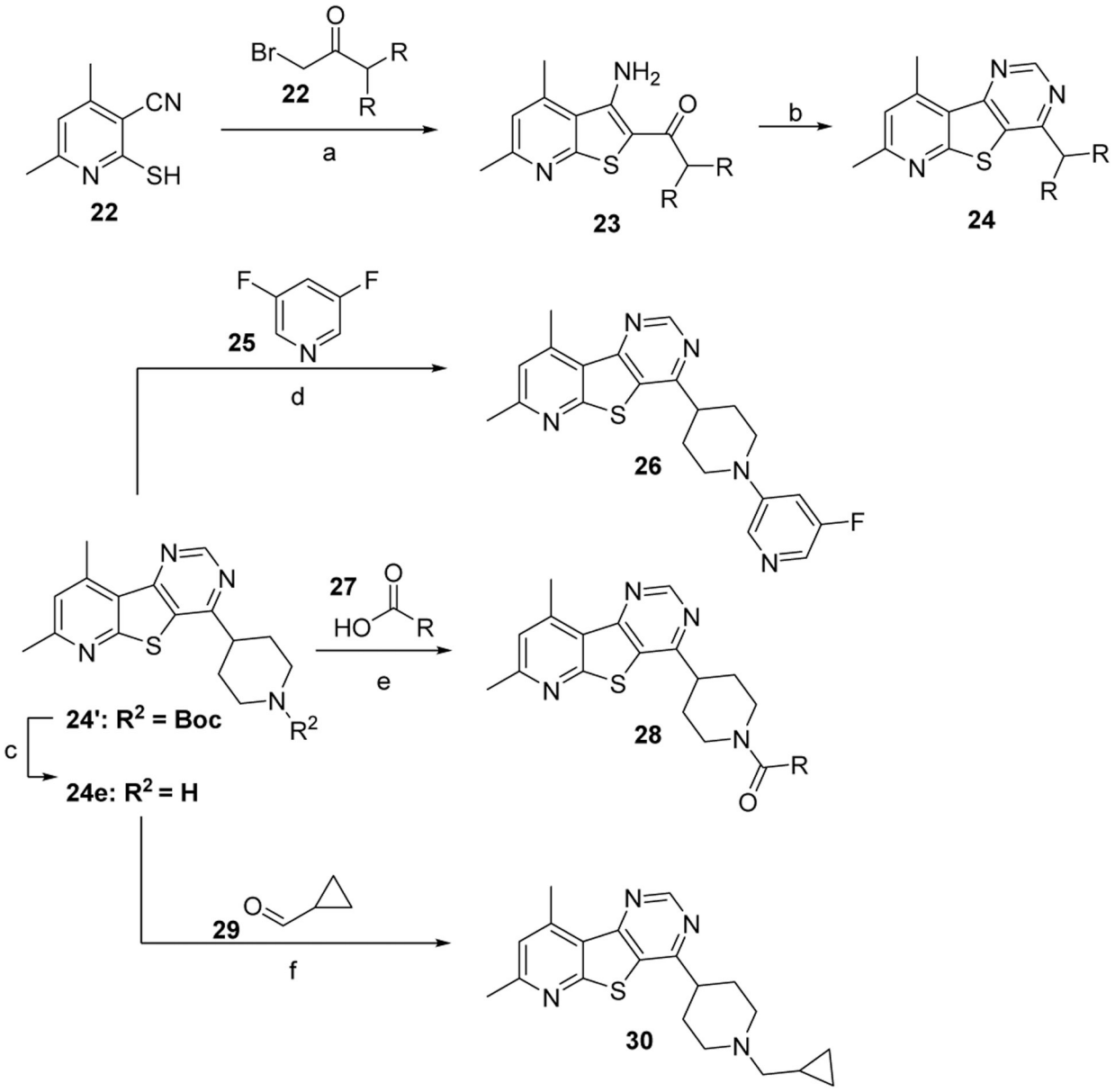

Scheme 2.

Synthesis of M_4 PAM analogs. Reagents and conditions: (a) **22**, KOH, IPA, 105 °C, 10–74%; (b) i. $HCONH_2$, 150 °C; ii. AcOH • $HN{=}CHNH_2$, 150 °C, 62 – 95%; (c) HCl, 1,4-dioxane/H_2O (1:1), 79%; (d) **25**, DIEA, NMP, 120 °C, 72h, 92%; (e) **27**, HATU, DIEA, DMF, 54–62%; (f) **29**, STAB. AcOH, DCM, 18h, 95%.

Table 1.

Structures and activities for analogs **16** & **19**.

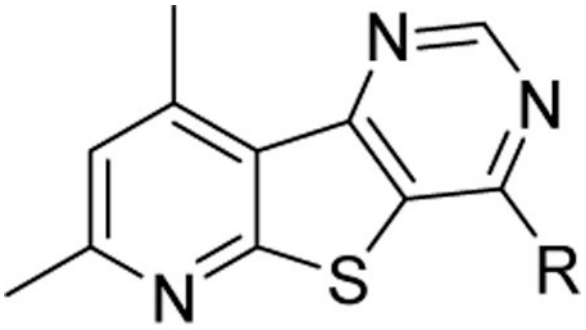

16 or 19

Cmpd	R Group	hM_4 EC_{50} (nM)[a] [%ACh Max]
16a **VU6008258**	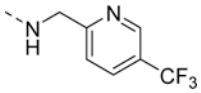	Inactive
16b **VU6008243**	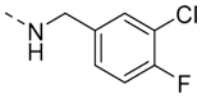	Inactive
16c **VU6008261**	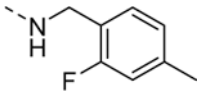	Inactive
16d **VU6008266**	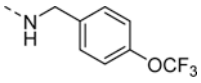	Inactive
16e **VU6008279**	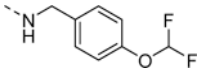	4,010 [45]
16f **VU6008248**	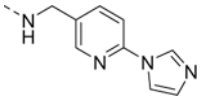	1,560 [34]
16g **VU6008250**	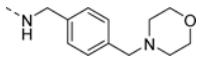	1,110 [47]
16h **VU6008255**	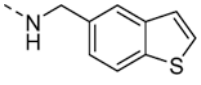	Inactive

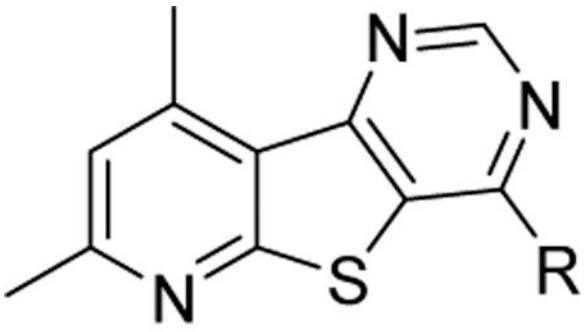

16 or 19

Cmpd	R Group	hM_4 EC_{50} (nM)[a] [%ACh Max]
16i **VU6008257**	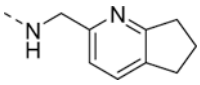	2,560 [30]
16j **VU6008256**	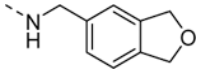	1,140 [41]
16k **VU6008254**	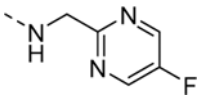	>10,000 [30]
16l **VU6008283**	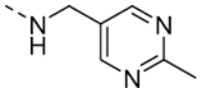	1,400 [54]
16m **VU6008284**	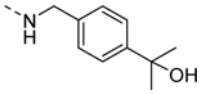	910 [76]
16n **VU6010076**	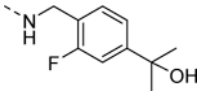	2,320 [74]
16o **VU6008280**	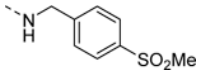	293 [42]
16p **VU6008452**	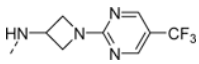	6,550 [52]
16q **VU6007221**	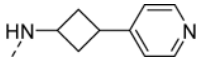	341 [67]
16r **VU6008278**	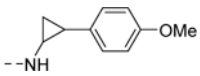	1,640 [61]

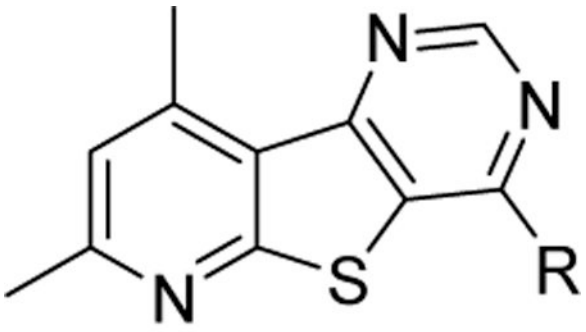

16 or 19

Cmpd	R Group	hM_4 EC_{50} (nM)[a] [%ACh Max]
19 **VU6010153**	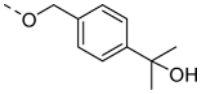	8,740 [40]

[a]Calcium mobilization assays with $hM_4/Gqi5$-CHO cells performed in the presence of an EC_{20} fixed concentration of acetylcholine, n =1 independent experiment in triplicate.

Table 2.

Structures and activities for analog **16** containing small aliphatic amines.

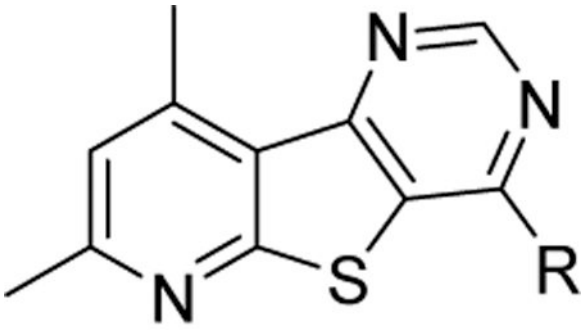

16

Cmpd	R Group	hM_4 EC_{50} (nM)[a] [%ACh Max]
16s **VU6007214**	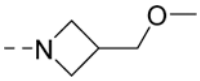	762 [50]
16t **VU6007218**	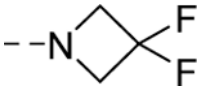	456 [69]
16u **VU6007216**	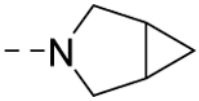	453 [75]
16v **VU6007220**	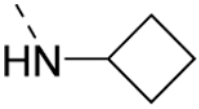	359 [76]
16w **VU6007219**	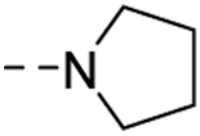	277 [67]
16x **VU6007217**	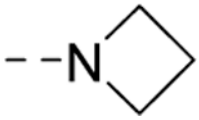	172 [59]
16y **VU6007215**		144 [84]

[a]Calcium mobilization assays with $hM_{4/Gqi5}$-CHO cells performed in the presence of an EC_{20} fixed concentration of acetylcholine, n =1 experiment performed in in triplicate.

Table 3.

Structures and activities for C-linked analogs **21**, **26, 28,** & **30**.

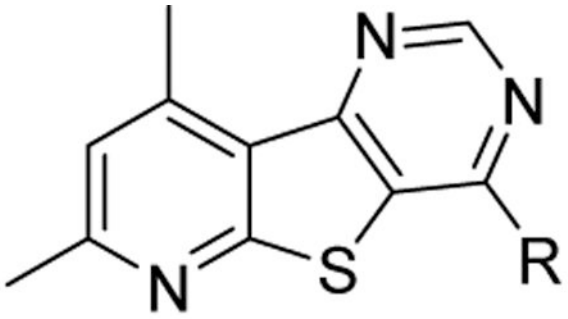

21, 24, 26, 28, or **30**

Cmpd	R Group	hM_4 EC_{50} (nM)[a] [%ACh Max]
24a **VU6008673**	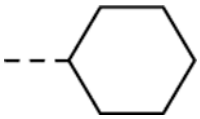	6,790 [71]
24b **VU6008479**	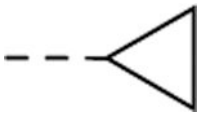	3,900 [62]
24c **VU6008362**	--CH_3	2,820 [58]
24d **VU6008676**	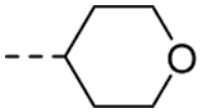	152 [99]
24e **VU6009094**	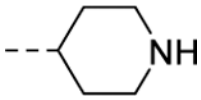	6,110 [44]
28a **VU6009098**	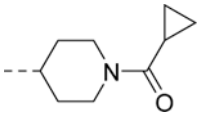	620 [62]
28b **VU6009100**	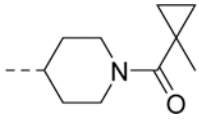	234 [72]

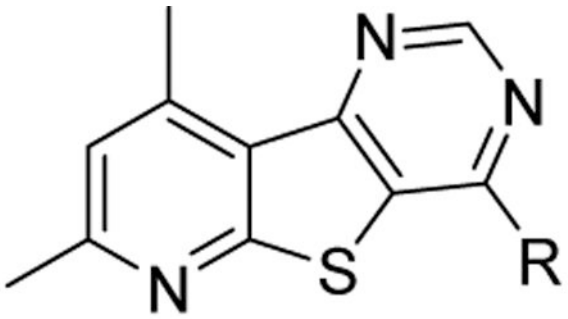

21, 24, 26, 28, or 30

Cmpd	R Group	hM_4 EC_{50} (nM)[a] [%ACh Max]
30 **VU6009198**	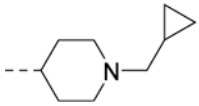	Inactive
26 **VU6009197**	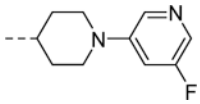	Inactive
21 **VU6007227**	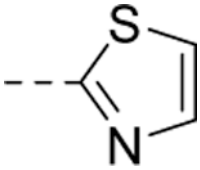	3,410 [62]

[a]Calcium mobilization assays with hM_4/Gqi5-CHO cells or performed in the presence of an EC_{20} fixed concentration of acetylcholine, n =1 independent experiment performed in triplicate.

Table 4.

Structures and activities for analog 17.

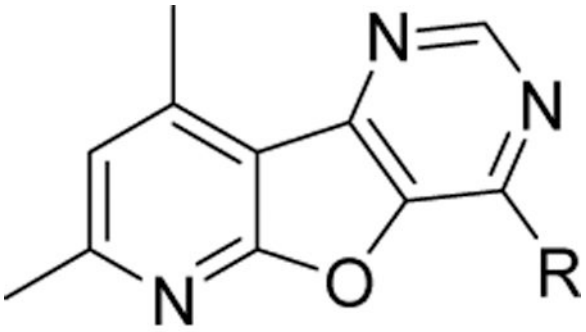

17

Cmpd	R Group	hM_4 EC_{50} (nM)[a] [%ACh Max]
17a **VU6008413**	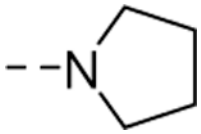	Inactive
17b **VU6008838**	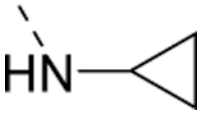	2,600 [64]
17c **VU6008833**	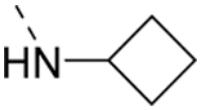	1,590 [44]
17d **VU6008822**	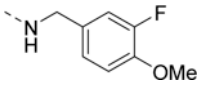	Inactive
17e **VU6009080**	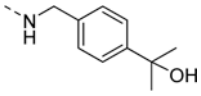	Inactive
17f **VU6008669**	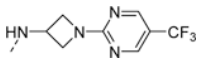	Inactive
17g **VU6008806**	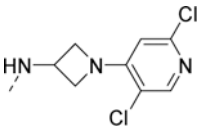	1,490 [49]

[a]Calcium mobilization assays with $hM_{4/Gqi5}$-CHO cells performed in the presence of an EC_{20} fixed concentration of acetylcholine, n =1 independent experiment performed in triplicate.

Table 5.

Structures and activities for analog 1**8**.

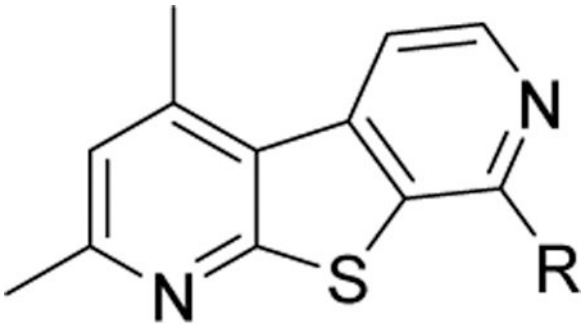

18

Cmpd	R Group	hM_4 EC_{50} (nM)[a] [%ACh Max]
18a **VU6010206**	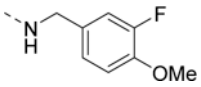	>10,000 [90]
18b **VU6010225**	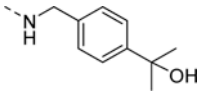	327 [101]
18c **VU6010205**	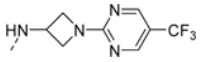	150 [80]
18d **VU6008889**	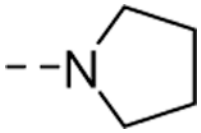	233 [98]
18e **VU6009049**	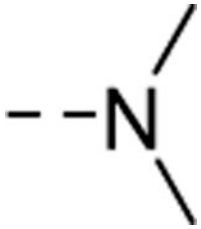	202 [82]
18f **VU6009203**	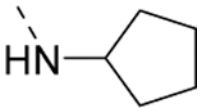	124 [71]
18g	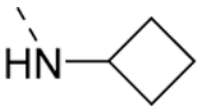	85

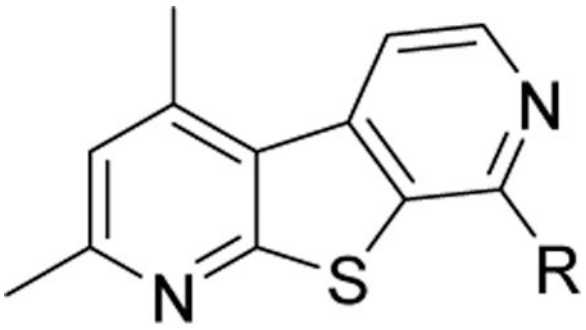

18

Cmpd	R Group	hM_4 EC_{50} (nM)[a] [%ACh Max]
VU6009048		[90]

[a]Calcium mobilization assays with hM_4/Gqi5-CHO cells performed in the presence of an EC_{20} fixed concentration of acetylcholine, n =1 independent experiment performed in triplicate.

Table 6.

In vitro DMPK and rat PBL data for select analogs **16, 18** & **28**.

Property	16o VU6008280	16w VU6007219	16x VU6007217	16y VU6007215	28b VU6009100	18b VU6010225	18d VU6008889	18g VU6009048
MW	398.5	284.38	270.35	312.39	380.51	377.5	283.39	283.39
xLogP	3.39	3.24	2.79	1.85	3.75	4.89	3.69	3.92
TPSA	84.8	41.9	41.9	51.1	59	58	29	37.8
***In vitro* PK parameters**								
CL_{INT} (mL/min/kg), rat	176	1896	741	594	367	334	2098	3859
CL_{HEP} (mL/min/kg), rat	50	68	64	63	59	58	68	69
CL_{INT} (mL/min/kg), human	28	134	296	129	25	50	161	345
CL_{HEP} (mL/min/kg), human	12	18	20	18	11	15	19	20
Rat fu_{plasma}	0.024	0.054	0.071	0.206	0.017	0.005	0.016	0.009
Human fu_{plasma}	0.002	0.016	0.021	0.056	0.017	0.001	0.003	0.005
Rat fu_{brain}	0.011	0.004	0.009	0.019	0.011	0.003	0.002	0.004
Brain Distribution (0.25 h) (SD Rat; 0.2 mg/kg IV)								
$K_{p,\ brain:plasma}$	0.45	5.36	6.49	4.47	0.54	2.27	37.1	10.4
$K_{puu,\ brain:plasma}$	0.21	0.65	0.27	0.40	0.35	1.16	4.87	4.18